Explicit vs Implicit Modelling of Refraction in Underwater Structure-from-Motion – A practical Guide

Fabio Menna[1,2], Robin Rofallski[3], Erica Nocerino[4]

[1] Department of Chemical, Physical, Mathematical and Natural Sciences, University of Sassari, Italy – fmenna@uniss.it
[2] Department of Science and Technology, University of Napoli Parthenope, Napoli, Italy
[3] Institute for Applied Photogrammetry and Geoinformatics, Jade University of Applied Sciences, Oldenburg, Germany robin.rofallski@jade-hs.de
[4] Department of Humanities and Social Sciences, University of Sassari, Sassari, Italy - enocerino@uniss.it

Keywords: Underwater Photogrammetry, Structure-from-Motion, Camera Calibration, Refraction, Simulation, Rendering.

Abstract

This study presents a critical investigation, based on computer simulations, of refractive Structure-from-Motion (SfM) methods for underwater photogrammetry. The goal is to provide practical guidelines on when explicit refractive modeling is necessary and when it can be safely neglected for a given application. Simulations are run within the POSER framework (https://github.com/GEOSS-UNISS/POSER), which uses the physical based rendering engine of Blender to model the physical properties of water, including light refraction, scattering, and absorption phenomena. Simulated camera configurations range from a GoPro with a fisheye lens in a flat-port housing to a full-frame machine vision camera in a housing equipped with a dome port. Different offsets between the camera centre and the port geometry are also introduced to represent both standard and non-conventional housing setups, including misalignments. The study compares refractive and implicit (standard) modelling approaches, evaluating their respective advantages and limitations in terms of parameter estimability, the need for pre-calibration, and the availability of ground control points. Accuracy is assessed against ground-truth simulated data by analysing discrepancies in reconstructed 3D geometry and exterior orientation parameters.

1. Introduction

1.1 Distance dependent systematic errors with flat and uncentred dome ports

In underwater photogrammetry, cameras are typically enclosed in waterproof housings equipped with either flat or hemispherical dome ports. As light passes through these interfaces, it is refracted at the water–port boundary, thereby violating the pinhole camera assumption that generally holds for standard above-water photogrammetric applications.

More specifically, systematic, distance-dependent errors (Maas, 1992) arise when the perspective centre—represented by the entrance pupil (EP) of the optical system—is not located on the flat interface (Łuczyński et al., 2017; Menna et al., 2018), or when the EP is not concentric with the hemispherical dome surface (Menna et al., 2020; She et al., 2022). In such cases, if the object-to-camera distance remains constant underwater and the surveyed object has limited three-dimensional extent within the camera's field of view, these systematic errors can be partially compensated by applying camera calibration parameters derived from the standard Brown–Beyer functional model (Gruen and Beyer, 2001).

Dome ports, when properly centred on the entrance pupil, are well suited for underwater photogrammetry, as they largely eliminate the geometric effects of refraction and preserve the camera's field of view. They are particularly advantageous for deep-water surveys due to their shape, which better withstands high pressure. However, they introduce additional optical challenges, such as the formation of a virtual image close to the dome and aberrations like Petzval curvature, which require careful camera setup. Compared to flat ports, they generally provide superior image quality and are the preferred choice for wide-angle lenses (Menna et al., 2016).

1.2 Implicit compensation vs explicit modelling of refraction

The presence of refraction-induced systematic errors has long been a major concern in underwater photogrammetry, prompting extensive investigations through both simulations (Menna et al., 2020; Rofallski et al., 2022) and real image datasets to assess the achievable accuracy of underwater measurements (Shortis, 2015). In parallel, several studies have proposed different approaches for either rigorous explicit modelling or implicit compensation of these effects (Kotowski, 1988; Jordt-Sedlazeck and Koch, 2013; Bräuer-Burchardt et al., 2016; Chadebecq et al., 2017; Nocerino et al., 2021; Rofallski and Luhmann, 2022; She et al., 2024).

In previous studies, the authors examined the influence of optical alignment and camera setup on underwater camera calibration using both real and simulated images. We focused on the differences between dome and flat ports, as well as on whether, in practical applications, the simplicity of implicitly modelling refraction can be prioritized over the rigor of extended camera models. To enable the use of standard photogrammetric software, Nocerino et al. (2021) proposed an iterative lookup-table-based polynomial correction of systematic image residuals within the bundle adjustment. The approach is agnostic to whether a dome or flat port is used and is effective whenever a systematic distance-dependent component is present in the image residuals.

Modelling the water refraction in underwater photogrammetry requires specialized software, traditionally developed within research domain. Using an appropriate functional model, refractive effects can be estimated through self-calibration as part of the bundle adjustment (BA) solution. However, not all camera

https://doi.org/10.5194/isprs-archives-XLIX-B2-2026-971-2026

network geometries are suitable for this task. Due to the increased number of parameters to be estimated, numerical instability and convergence issues are common. Moreover, strong parameter correlations arise, for example between the principal distance *c*, the refractive index, and the offset of the refractive surface (i.e., the flat interface or the dome centre relative to the entrance pupil) (Rofallski et al., 2025). Reliable estimation therefore requires ad hoc calibration setups, with optimized camera network geometries, and calibration object known with high accuracy, which are not always practical in real underwater applications.

1.3 Refractive SfM

More recently, COLMAP (Schonberger & Frahm, 2016) has been extended in an open-source implementation to rigorously model refractive surfaces within a Structure-from-Motion (SfM) framework (She et al., 2024). This approach integrates refraction effects for both flat and dome ports into image orientation and bundle adjustment. Unlike the implicit approach that uses a standard pinhole model extended with in plane distortion parameters to account for the refraction, this approach incorporates physical refraction at water–glass–air interfaces directly into image formation, camera pose estimation, and bundle adjustment. It supports both flat and dome port interfaces, enabling geometrically accurate reconstructions in underwater environments.

1.4 Aim of the paper

This work extends the authors' previous studies by introducing new simulations specifically aimed at practical underwater applications using commonly adopted sensors and configurations. The simulated camera systems range from action cameras, such as GoPro-like action cameras equipped with standard flat-port housings widely used by marine ecologists and archaeologists, to full-frame machine vision cameras within dome ports. In addition, varying offsets from the flat interface and dome centre are considered to simulate both standard and non-conventional housings with suboptimal setups. The study provides a critical investigation aimed at establishing practical guidelines for determining when additional refractive parameters are necessary and when they can be neglected for the application of interest. In our study, the generated images are photogrammetrically processed following different approaches:

a) a standard pinhole camera modelling with additional in plane distortion parameters and,
b) a rigorous approach that extends it with explicit modelling of refraction.

We investigate the benefits and cons of the refractive vs the implicit modelling approaches with respect to estimability of camera calibration (refractive) parameters, need for pre-calibration setups, availability of ground control points, and assessing the accuracy of both approaches against ground truth simulated data. Agisoft Metashape (https://www.agisoft.com/) and COLMAP are used for testing approach (a), the refractive version of COLMAP is tested for experimenting with approach (b). The accuracy is reported as discrepancies in the reconstructed 3D models and exterior orientation.

2. Material and Methods

2.1 Refractive SfM datasets in POSER

We utilize the POSER framework (https://github.com/GEOSS-UNISS/POSER) (Menna et al., 2024) developed within the 2024 ISPRS Education and Capacity Building Initiatives (ECBI). POSER uses the physical based rendering engine of Blender (https://www.blender.org/) to generate synthetic image datasets with realistic modelling of the physical properties of water, including light refraction, scattering, and absorption phenomena, to simulate underwater surveying conditions (Figure 1).

Figure 1. Blender interface showing one of the educational scenes used for underwater photogrammetry simulations within the POSER 2024 ISPRS Education and Capacity Building Initiatives (ECBI)

The simulated underwater scenes (Table 1) cover different applications:

1. A calibration setup with redundant camera network mixing coded targets and random pattern for classical feature extraction and matching of interest points;
2. an underwater archaeological site in shallow water;
3. a large rectangular plot for the ecological monitoring of a benthic coral reef habitat;
4. a subsea metrology underwater scene acquired in deep sea by an ROV, following a "corridor" like image acquisition schema.

The calibration dataset uses a CAD model of an updated version of the test object with 160 circular coded targets used in Menna et al (2016) with the inclusion of random pattern patches.

Dataset	Size [m^2]	Camera Type	Lens	Port Interface	# Photos | Simulated Image resolution	Distance from the Seabed [m] | GSD [mm]
1 - calibration	1.5x1	Action Camera – GoPro Hero 10	Fisheye equisolid 2.9mm	Flat	200 | 6MP	0.75 | 0.2
2 – columns	12x9	Action Camera – GoPro Hero 10	Fisheye equisolid 2.9mm	Flat	250 | 6MP	1.90 | 1.1
3 – coral reef	56x10	Consumer underwater– OM system TG7	Rectilinear 4.3 mm	Flat	1000 | 12MP	3.6 | 1.3
4- pipeline	70x60	Full Frame machine Vision	Rectilinear 20.0 mm	Dome	2000 | 6MP	1.7 | 1.0

Table 1. Main characteristics of the simulated datasets.

Dataset
1)
2)
3)
4)

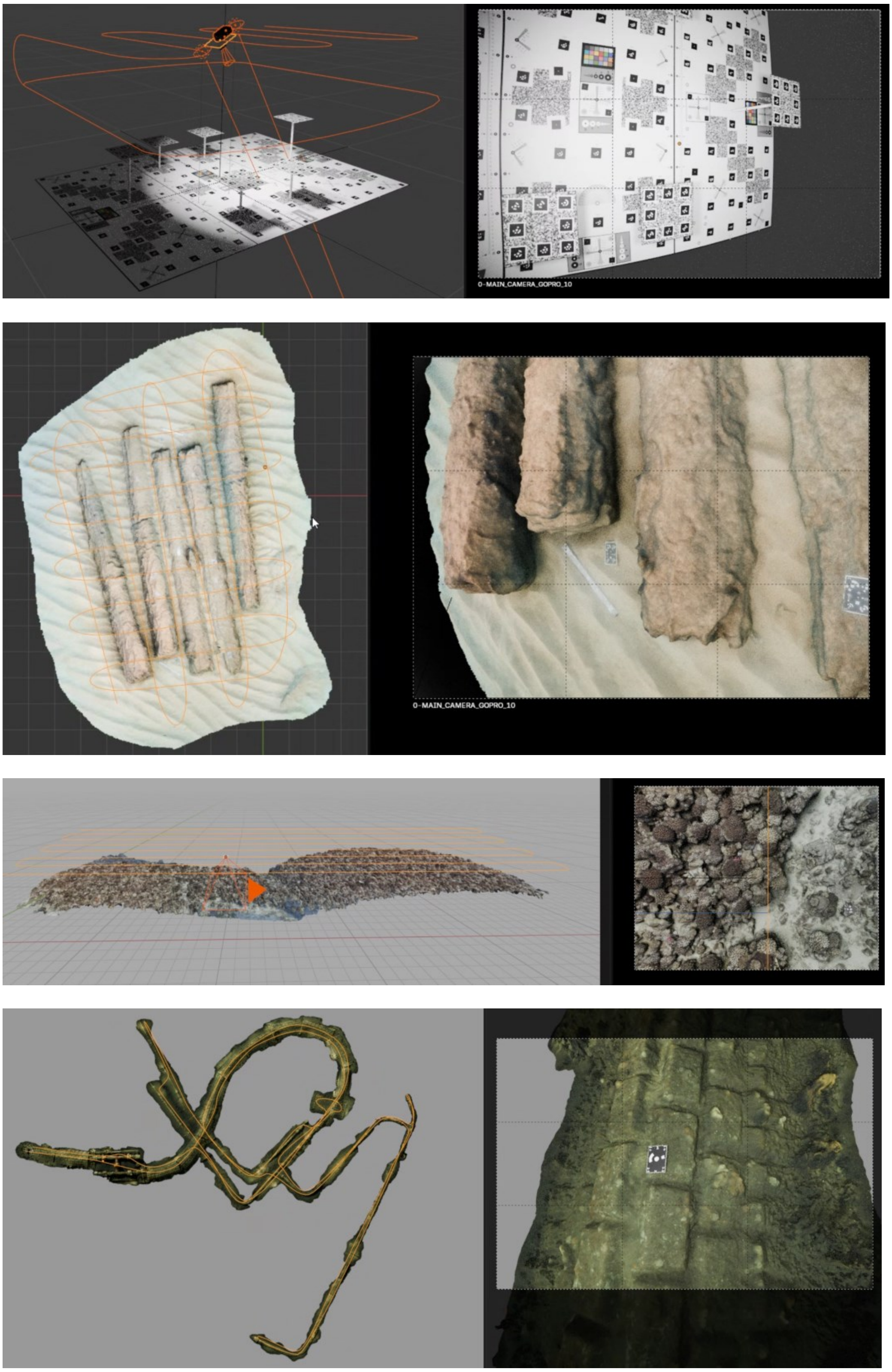

Figure 2. 3D models and examples of rendered scenes from the POSER project used in this study.

Figure 3. Simulated optical systems ranging from action (GoPro 10 – left), compact (OM system TG7 - centre), and full frame machine vision (e.g. similar to the 3000 m depth rated ORUS 3D® trinocular sensor (Menna et al., 2019) , now IVM technologies - www.ivm-technologies.com/) cameras.

The remaining datasets are all simulated starting from 3D models produced with underwater photogrammetry in real-case projects. Further technical details about the simulated datasets are provided in Table 1. Representative images of the simulated datasets are shown in Figure 2.

We simulated three different underwater camera systems (Figure 3). The nominal camera calibration parameters, and the flat and dome port offsets were taken from datasheets or measured in laboratory. The simulated systems were:

a) GoPro10 action camera (Figure 3 – left) with standard housing. We considered a thickness of 2mm for the flat interface on the external housing and 2mm for the one on camera body, respectively. The offset from the EP to the waterproof housing flat interface was estimated to be about 5mm.
b) OM system TG7 compact camera with underwater housing featuring a flat port (Figure 3 – centre). We estimated an offset of 10 mm and thickness of 8mm of the flat port.
c) Machine vision camera with dome port (Figure 3 – right). We used nominal parameters (inner radius 75mm, external radius 85mm) for a typical small sized dome for a full frame sensor.

For all the simulations we used the measured values or more penalizing setups, for example from thicker housings needed in deep waters that may represent the boundary conditions under which an explicit refraction model becomes necessary. The images were rendered using Cycles rendering from Blender with no distortion synthetically added to the images. Therefore, any resulting image distortion is only due to either the fisheye projection or refraction at port interfaces. The refraction coefficients for air, glass and water were set to 1.0, 1.47, 1.33, respectively.

2.2 Photogrammetric processing

A workstation computer with Intel® Core ™ i7-14700K processor and a 16GB NVIDIA GeForce RTX 4080 SUPER graphic card was used to process the simulated datasets with Windows 11 Pro operating system. Agisoft Metashape and COLMAP were used to orient the images in a free network solution following a classical SfM workflow using standard Brown parameters including radial and tangential distortions with the aim to compensate for longitudinal and lateral offsets. Images were processed at full resolution in Metashape.

Refractive Structure-from-Motion (SfM) was performed using COLMAP refractive within the Windows Subsystem for Linux (WSL 2). WSL 2 provides a full Linux kernel inside Windows, enabling execution of Linux-native software while allowing direct access to the Windows file system. This setup avoids the need for dual-booting or heavy virtual machines and facilitates installation of dependencies and libraries required by COLMAP.

GPU acceleration was enabled through NVIDIA CUDA support in WSL 2, allowing COLMAP to leverage the graphics card for feature extraction and matching. Input data stored on the Windows filesystem were accessed via WSL-mounted drives, and for performance-critical operations, data were temporarily copied to the Linux filesystem to maximize I/O efficiency. This configuration enables efficient 3D reconstruction directly from a Windows workstation.

The refractive version of COLMAP requires that the flat and dome port parameters be provided as initial approximation for the refractive SfM to run. The parameters are used throughout the feature extraction, matching and image orientation stages. An example of graphical user interface in COLMAP refractive showing the flat port parameters such as plane orientation (its normal Nx, Ny, Nz), internal distance from the EP, thickness and refractive indices of air, glass and water is shown in Figure 4.

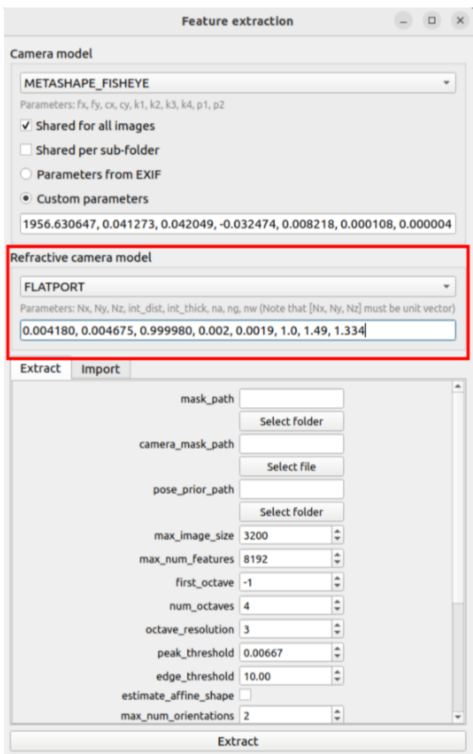

Figure 4. COLMAP GUI to input the approximate refractive parameters for a flat port (https://github.com/the-sauer/colmap_underwater)

<table>
<tr><th></th><th></th><th></th><th></th><th colspan="4">TARGET CHECKPOINT ERRORS [mm]</th><th colspan="3">CAM POSITION ERRORS [mm]</th></tr>
<tr><th></th><th></th><th></th><th></th><th>X</th><th>Y</th><th>Z</th><th></th><th>X</th><th>Y</th><th>Z</th></tr>
<tr><th>Dataset processing version |</th><th>Refraction modelling</th><th>Self Calibration</th><th>RMS [px]</th><th>RMS| min |max</th><th>RMS| min |max</th><th>RMS| min |max</th><th>RMS [px] targets</th><th>RMS| min |max</th><th>RMS| min |max</th><th>RMS| min |max</th></tr>
<tr><td>1a - calibration EP10mm, Thickn02mm</td><td>Implicit Rectilinear Brown – Metashape f, cx, cy, k1-4, p1, p2</td><td>Yes, all parameters</td><td>0.7</td><td>0.06 | -0.03 | 0.02</td><td>0.03 | -0.06 | 0.08</td><td>0.1| -0.2 | 0.2</td><td>0.9</td><td>-</td><td>-</td><td>-</td></tr>
<tr><td>1b -calibration EP50mm, Thickn02mm</td><td>Implicit Rectilinear Brown – Metashape f, cx, cy, k1-4, p1, p2</td><td>Yes, all parameters</td><td>1.8</td><td>0.2 | -0.7 | 0.7</td><td>0.1 | -0.3 | 0.2</td><td>0.4 | -0.7 | -0.9</td><td>4.5</td><td>-</td><td>-</td><td>-</td></tr>
<tr><td>2a – columns EP20 mm, Thickn10 mm</td><td>Implicit Rectilinear Brown – Metashape f, cx, cy, k1-4, p1, p2</td><td>Yes, all parameters</td><td>0.6</td><td>-</td><td>-</td><td>-</td><td>-</td><td>1.4 | -2.5 | 2.6</td><td>0.8 | -2.6 | 2.8</td><td>3.2 | -4.8 | 9.9</td></tr>
<tr><td>2b – columns EP20 mm, Thickn10 mm</td><td>Explicit, Fisheye, COLMAP refractive SfM</td><td>Yes, all parameters including refractive</td><td>-</td><td>-</td><td>-</td><td>-</td><td>-</td><td>0.2 | - | -</td><td>0.2 | - | -</td><td>0.2 | - | -</td></tr>
<tr><td>2c – columns EP20 mm, Thickn10 mm</td><td>Implicit Rectilinear Brown – Metashape f, cx, cy, k1-4, p1, p2 constrained on COLMAP refractive cam positions from 2b</td><td>Yes, all parameters</td><td>0.8</td><td>-</td><td>-</td><td>-</td><td>-</td><td>0.2 | -1.5 | 0.7</td><td>0.2 | -0.4 | 1.2</td><td>0.2| -0.7 | 0.4</td></tr>
<tr><td>3a – Moorea EP50 mm, Thickn8 mm</td><td>Implicit Simple Radial – COLMAP f, cx, cy, k1</td><td>Yes, all parameters</td><td>-</td><td>-</td><td>-</td><td>-</td><td>-</td><td>18.4 | -24.9 | 112.0|</td><td>38.9 | -141.7 | 61.9</td><td>183.4 | -220.8 | 470.3</td></tr>
<tr><td>3b – Moorea EP50 mm, Thickn8 mm</td><td>Explicit Simple Radial – COLMAP refractive, f, cx, cy, k1, Nx, Ny, Nz, EPoffset</td><td>Yes, camera and flat parameters</td><td>-</td><td>-</td><td>-</td><td>-</td><td>-</td><td>0.9 | -4.1 | 2.9</td><td>0.8 | -2.9 | 2.2</td><td>6.7 | -17.0 | 8.6</td></tr>
<tr><td>3c – Moorea EP50 mm, Thickn8 mm</td><td>Implicit Rectilinear Brown – Metashape f, cx, cy, k1-4, p1, p2</td><td>Yes, all parameters</td><td>0.3</td><td>-</td><td>-</td><td>-</td><td>-</td><td>12.0 | -19.6 | 21.8</td><td>7.2 | -20.1 | 16.3</td><td>30.4 | -45.0 | 0.082</td></tr>
<tr><td>3d – Moorea EP50 mm, Thickn8 mm</td><td>Implicit Rectilinear Brown – Metashape f, cx, cy, k1-4, p1, p2 constrained on COLMAP refractive cam positions from IIIb</td><td>Yes, all parameters</td><td>0.4</td><td>-</td><td>-</td><td>-</td><td>-</td><td>0.9 | -4.1 | 2.7</td><td>1.1 | -2.9 | 3.3</td><td>5.8 | -15.4 | 7.2</td></tr>
<tr><td>3e – Moorea EP10 mm, Thickn8 mm</td><td>Implicit Rectilinear Brown – Metashape f, cx, cy, k1-4, p1, p2</td><td>Yes, all parameters</td><td>0.3</td><td>-</td><td>-</td><td>-</td><td>-</td><td>2.2 | -3.7 | 4.1</td><td>1.3 | -3.5 | 2.9</td><td>5.7 | -8.5 | 15.3</td></tr>
<tr><td>4a - pipeline EPZ(forward) 20mm, EPX(lateral) 10mm</td><td>Implicit Rectilinear Brown – Metashape f, cx, cy, k1-3, p1, p2</td><td>Yes, all parameters</td><td>0.4</td><td>108.8 | -111.7 | 204.8</td><td>104 | -192.0 | 146.6</td><td>198 |-203.4 | 352.5</td><td>0.8</td><td>80.8 | -189.9 | 183.1</td><td>92.2 | -273.5 | 189.0</td><td>214.1 | -273.3 | 395.7</td></tr>
<tr><td>4b - pipeline EPZ(forward) 20mm, EPX(lateral) 10mm</td><td>Explicit, Pinhole, COLMAP refractive SfM</td><td>No, all precalibrated</td><td>-</td><td>-</td><td>-</td><td>-</td><td>-</td><td>11.6 | -16.3 | 27.2</td><td>10.4 | -22.8 | 38.6</td><td>10.0 | -35.1 | 37.8</td></tr>
<tr><td>4c - pipeline EPZ(forward) 20mm, EPX(lateral) 10mm</td><td>Explicit, Pinhole, COLMAP refractive SfM</td><td>Yes, refractive parameters (dome centre)</td><td>-</td><td>-</td><td>-</td><td>-</td><td>-</td><td>52.6| -151.4| 138.9</td><td>43.1| -114.5 | 118.9</td><td>209.4 |-677.4 | 318.5</td></tr>
<tr><td>4d - pipeline EPZ(forward) 20mm, EPX(lateral) 10mm</td><td>Explicit, Pinhole, COLMAP refractive SfM</td><td>Yes, all interior and refractive parameters (dome centre)</td><td>-</td><td>-</td><td>-</td><td>-</td><td>-</td><td>100.9 | -306.0 | 271.8</td><td>101.2 | -300.7 | 239.8</td><td>226.5 | -811.9 | 289.9</td></tr>
</table>

Table 2. Different processing results for the implicit and explicit modelling of refraction with the 4 simulated scenes.

These parameters need to be known a priori with a good approximation and preferably calibrated using the Calibmar tool (Seegräber, 2024, https://cau-git.rz.uni-kiel.de/inf-ag-koeser/calibmar). In our tests we always started from the known calibration parameters used for rendering in POSER.

After the SfM process we exported the image orientation parameters and compared the camera positions with the ground truth values from POSER after applying a similarity transformation with isotropic scale factor. For the datasets 1 and 4, intended for more metrological applications, we also compared the coordinates of coded targets available within the scene as check points.

For all the datasets, the coordinate reference system (CRS) had the OXY plane horizontal, with the X axis aligned along the main object direction and Z up.

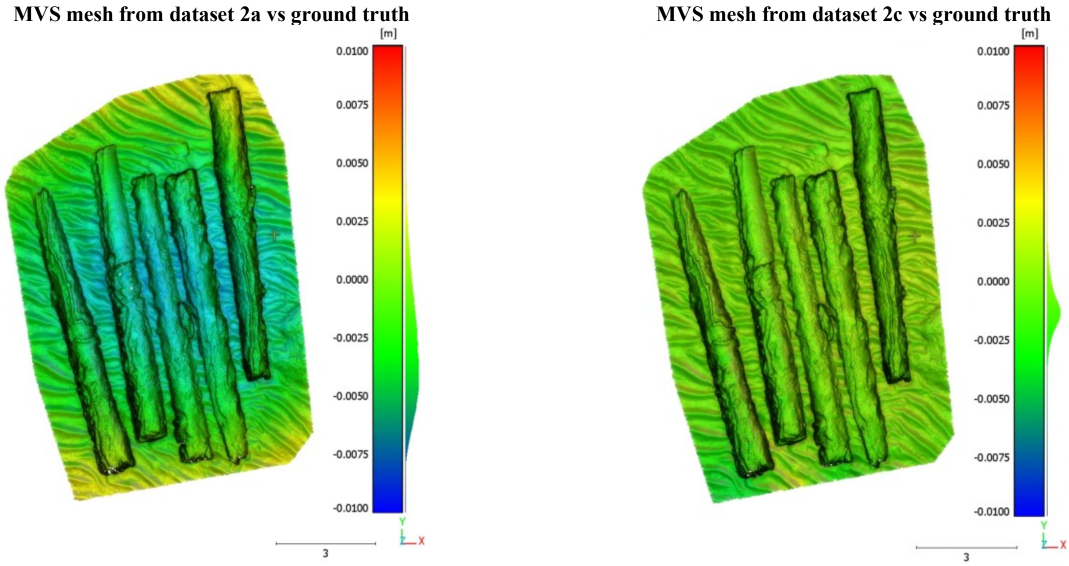

Figure 5. Multi view stereo (MVS) 3D mesh reconstruction as computed in Metashape and compared to the ground truth 3D mesh model used in Blender for the simulation in the dataset version 2a (left) and 2c (right), respectively.

3. Results and Discussion

3.1 Refractive aware vs implicit modelling analyses

Table 1 summarizes the results of different SfM runs performed using Agisoft Metashape, COLMAP, and COLMAP Refractive. Only the most relevant results are reported, as they support the following discussion and provide practical guidance—particularly for non-experts—on handling underwater camera systems and refractive datasets.

The main takeaway, consistent with previous studies (Menna et al., 2018, 2020; Nocerino et al., 2021; Rofallski et al., 2022), is that in many standard underwater housings the refractive offsets are sufficiently small for the classical Brown camera model to achieve adequate accuracy for many applications.

Dataset 1 is composed of 200 images taken around a three-dimensional test object with a typical camera calibration imaging network that includes convergent and rolled images using a GoPro 10 like action camera. Two distances are kept from the main object plane along the acquisition path. The oblique images provide significant distance variation within the field of view of the camera. The two results (1a, 1b) show that even in the case of a big flat to entrance pupil EP offset (50mm) the potential accuracy on the check points is still submillimetre. Unless higher accuracy is necessary, the classical Brown model may be still adequate in many practical situations.

Dataset 2 simulates the underwater photogrammetric documentation and monitoring of an archaeological site, more specifically, a shipwreck cargo consisting of five columns lying on a sandy seabed in shallow water (less than 6 meters). The imaging network consists of 250 photos with parallel and cross strips including oblique images that provided enough redundancy, symmetry and proper geometry able to mitigate systematic errors introduced by the flat port, placed at 20mm from the EP. The results of the SfM processing in Metashape shows sub-centimetre RMSE on the camera positions. This accuracy may be sufficient for most documentation and monitoring applications. It is worth noticing that the camera model uses the Brown formulation for a rectilinear lens. Indeed, the combination of the barrel distortion, typically visible with a fisheye lens and the pincushion distortion introduced by the flat port allows the two distortions compensate with each other making the GoPro images acting like a rectilinear lens model.
Moreover, for the same dataset, to simulate structural deformation monitoring, we tested the rigorous modelling of the flat port in COLMAP refractive. With proper modelling of the refraction, dataset 2b processing version shows sub-millimeter RMS residuals on the camera positions exported from COLMAP.

We added a supplementary hybrid processing step that integrates COLMAP refractive and Metashape by using the camera positions from dataset processing 2b as soft constraints (1mm spatial standard deviation) in the bundle adjustment (BA) in Metashape.

This allows to orient the images using a standard Brown model in Metashape but constraining them to more accurate camera position obtained from a BA that incorporates rigorous modelling of refraction. The results show a submillimetre accuracy potential. Also, this process allows to use all the available processing tools and photogrammetric data production workflow from Agisoft Metashape. Indeed, in Figure 5 the multi view stereo (MVS) 3D mesh reconstruction as computed in Metashape is compared to the ground truth 3D mesh model used in Blender for the simulation. The typical doming deformation arising from the absorption of systematic errors (processing version 2a – Figure 5- left)) is significantly mitigated in the processing version 2c (Figure 5 - right).

Dataset 3 simulates a big coral reef plot measuring 56x10 m^2 imaged with sub-centimetre GSD. The aim of this scenery is a long-term ecological monitoring (LTER) of the coral reef to track bleaching events and map in 3D the growth of the reef.
The results show that except for the suboptimal setup with the flat port at 50mm from EP, a standard housing with flat port (10mm offset) could be used for the task just described above, being the flat port errors within the sub-centimeter range. A further analysis carried out in CloudCompare (https://www.cloudcompare.org/) compares the tie points with the ground truth reference surface, confirming the limited doming effect (Figure 6).

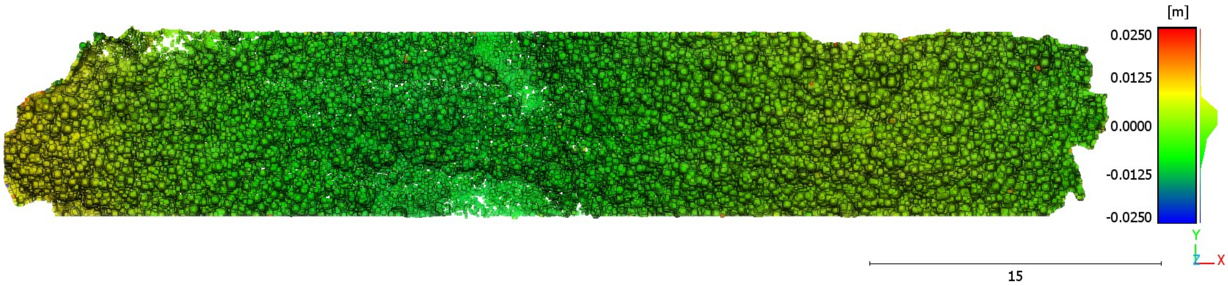

Figure 6. A 3D comparison between tie point from dataset processing version 3e and ground truth mesh model showing sub-centimetre errors introduced by the flat port when using an implicit modelling approach in Agisoft Metashape.

Dataset 4 simulates an Oil&Gas subsea metrology application, where an ROV inspects and surveys a deep-water pipeline. In this case, we used a dome port and a full frame sensor for best image quality, but introduced a significant misalignment of the dome port 2cm longitudinally along the optical axis and 1 cm laterally. In this case big errors in the order of a few decimetres arise with the implicit absorption, that would not likely fit the accuracy demands. Both RMSE on camera positions and check points show errors beyond 15cm. Similarly, the point to mesh distance analysis between the tie points and the reference mesh confirm the big doming systematic effect (Figure 7 - left). If the offsets are known through a calibration process, the error is greatly reduced in COLMAP refractive (processing 4b). However, refractive parameters are not accurately determinable in a simultaneous self-calibration adjustment with this dataset (processing 4c - only dome center, 4d – dome center and interior orientation parameters, Figure 7 - right), most probably due to the weak camera network geometry. Both RMSE on camera positions and comparison of the tie points with the ground truth model show maximum beyond 50cm, even worse than the implicit absorption approach.

4. Conclusion and future work

This study provided a critical assessment, based on computer simulations, of refractive Structure-from-Motion (SfM) methods for underwater photogrammetry, with the aim of offering practical guidelines on when explicit refractive modeling is required. The results show that, for typical underwater housings—such as a GoPro in a flat port or full-frame systems in dome ports with limited offsets—standard implicit models can often achieve sufficient accuracy for many applications. However, as misalignments and deviations from ideal configurations increase, refractive modeling becomes essential to avoid systematic errors in geometry and camera parameters.

The comparison between refractive and implicit approaches highlights a trade-off between model complexity and robustness. While refractive models provide improved physical consistency and accuracy under non-ideal conditions, they require careful calibration, appropriate network geometry, and, in some cases, additional constraints such as ground control points or pre-calibration. Overall, the findings emphasize that the choice of modeling approach should be guided by the specific acquisition setup and required accuracy, rather than adopting refractive modeling as a default solution.

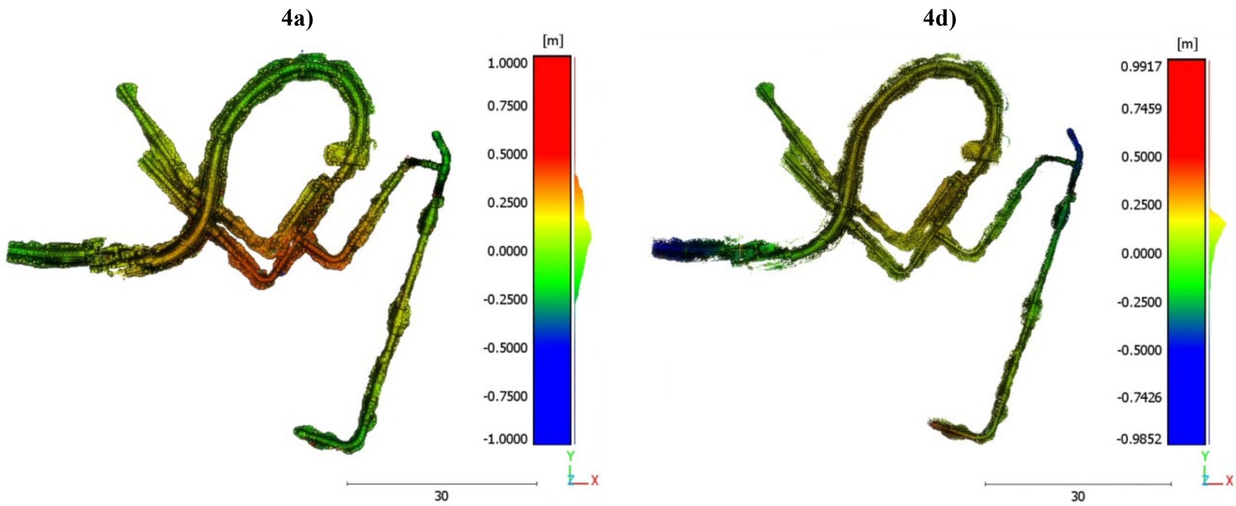

Figure 7. A 3D comparison between tie points from dataset processing version 4a (left) and ground truth mesh model showing big doming systematic effect when using an implicit modelling approach in Agisoft Metashape with a laterally decentred dome port. The refractive version of COLMAP can significantly reduce the errors by modelling these systematic errors (Table 2 processing 4b), but the calibration needs to be computed separately, with an ad hoc camera network. In this example (4d – right) self-calibration of refractive parameters does not improve significantly the implicit version (4a -left) with maximum absolute errors that reach almost 1m.

Acknowledgements

POSER is funded by the ISPRS ECBI 2024 program. The authors thank the team involved in the Moorea IDEA project (financial and scientific support of Prof. M. Troyer through the Institute of Theoretical Physics, ETH Zurich, the U.S. NSF under Grant No. OCE 16-37396 and earlier awards, and a generous gift from the Gordon and Betty Moore Foundation) for the Moorea dataset; IVM technologies for the subsea metrology dataset. The dataset of the columns was acquired within the second edition of the SUNRISE Summer School. The work was partially supported by "Paesaggi Archeologici Sommersi della Campania" project – PAS, MIMIT – CUP B69J25000050005. The authors acknowledge the use of ChatGPT (OpenAI) for assistance with English language editing and improving the clarity of the manuscript.

References

Bräuer-Burchardt, C., Heinze, M., Schmidt, I., Kühmstedt, P., Notni, G., 2016. Underwater 3D Surface Measurement Using Fringe Projection Based Scanning Devices. *Sensors*, 16(1), 13. https://doi.org/10.3390/s16010013

Chadebecq, F., Vasconcelos, F., Dwyer, G., Lacher, R., Ourselin, S., Vercauteren, T., Stoyanov, D., 2017. Refractive structure-from-motion through a flat refractive interface. In Proceedings of the IEEE international Conference on Computer Vision (pp. 5315-5323).

Gruen, A., Beyer, H., A., 2001. System calibration through self-calibration. In Calibration and orientation of cameras in computer vision (pp. 163-193). Berlin, Heidelberg: Springer Berlin Heidelberg.

Kotowski, R., 1988. Phototriangulation in multi-media photogrammetry. *Int. Arch. Photogramm. Remote Sens. Spatial Inf. Sci.*, 27, 324-334.

Jordt-Sedlazeck, A., Koch, R., 2013. Refractive structure-from-motion on underwater images. In Proceedings of the IEEE international Conference on Computer Vision (pp. 57-64).

Łuczyński, T., Pfingsthorn, M., Birk, A., 2017. The pinax-model for accurate and efficient refraction correction of underwater cameras in flat-pane housings. *Ocean Engineering*, 133, 9-22.

Maas, H. G. 1992. Digitale Photogrammetrie in der dreidimensionalen Strömungsmesstechnik (Doctoral dissertation, ETH Zurich).

Menna, F., Nocerino, E., Fassi, F., Remondino, F., 2016. Geometric and optic characterization of a hemispherical dome port for underwater photogrammetry. Sensors, 16(1), 48.

Menna, F., Nocerino, E., Remondino, F., 2017. Optical aberrations in underwater photogrammetry with flat and hemispherical dome ports. In Videometrics, Range Imaging, and Applications XIV (Vol. 10332, pp. 28-41). SPIE.

Menna, F., Nocerino, E., Drap, P., Remondino, F., Murtiyoso, A., Grussenmeyer, P., & Börlin, N., 2018. Improving underwater accuracy by empirical weighting of image observations. *The International Archives of the Photogrammetry, Remote Sensing and Spatial Information Sciences*, 42, 699-705.

Menna, F., Nocerino, E., Nawaf, M. M., Seinturier, J., Torresani, A., Drap, P., Remondino., F., Chemisky, B., 2019. Towards real-time underwater photogrammetry for subsea metrology applications. OCEANS 2019-Marseille, 1-10.

Menna, F., Nocerino, E., Ural, S., Gruen, A., 2020. Mitigating image residuals systematic patterns in underwater photogrammetry. *The International Archives of the Photogrammetry, Remote Sensing and Spatial Information Sciences*, 43, 977-984.

Menna, F., McAvoy, S., Nocerino, E., Tanduo, B., Giuseffi, L., Calantropio, A., Chiabrando, F., Teppati Losè, L., Lingua, A. M., Sandin, S., Edwards, C., Zgliczynski, B., Rissolo, D., and Kuester, F.: POSER: an oPen sOurce Simulation platform for tEaching and tRaining underwater photogrammetry, *Int. Arch. Photogramm. Remote Sens. Spatial Inf. Sci.*, XLVIII-2-2024, 265–272.

Nocerino, E., Menna, F., Grün, A., 2021. Bundle adjustment with polynomial point-to-camera distance dependent corrections for underwater photogrammetry. *The International Archives of the Photogrammetry, Remote Sensing and Spatial Information Sciences*, 43, 673-679.

Rofallski, R., Kahmen, O., Luhmann, T., 2022. Investigating distance-dependent distortion in multimedia photogrammetry for flat refractive interfaces. *The International Archives of the Photogrammetry, Remote Sensing and Spatial Information Sciences*, 48, 127-134.

Rofallski, R., Luhmann, T., 2022. An efficient solution to ray tracing problems in multimedia photogrammetry for flat refractive interfaces. *PFG–Journal of Photogrammetry, Remote Sensing and Geoinformation Science*, 90(1), 37-54.

Rofallski, R., Colson, A., Luhmann, T., 2025. Evaluating Interior Orientation Estimability in Multimedia Photogrammetry-A practical guide on object-invariant bundles. *The International Archives of the Photogrammetry, Remote Sensing and Spatial Information Sciences*, 48, 255-262.

Schonberger, J. L., & Frahm, J. M., 2016. Structure-from-motion revisited. In Proceedings of the IEEE conference on computer vision and pattern recognition (pp. 4104-4113).

Schonberger, J.L. and Frahm, J.M., 2016. Structure-from-motion revisited. In Proceedings of the IEEE conference on computer vision and pattern recognition (pp. 4104-4113).

Seegräber, F., She, M., Woelk, F., Köser, K., 2024. A Calibration Tool for Refractive Underwater Vision. arXiv preprint arXiv:2405.18018.

She, M., Nakath, D., Song, Y., Köser, K., 2022. Refractive geometry for underwater domes. *ISPRS Journal of Photogrammetry and Remote Sensing*, 183, 525-540.

She, M., Seegräber, F., Nakath, D., Köser, K., 2024. Refractive COLMAP: refractive structure-from-motion revisited. *In 2024 IEEE/RSJ International Conference on Intelligent Robots and Systems (IROS)* (pp. 12816-12823). IEEE.

Shortis, M., 2015. Calibration techniques for accurate measurements by underwater camera systems. *Sensors*, 15(12), 30810-30826.